http://dx.doi.org/10.5935/0103-5053.20130157

J. Braz. Chem. Soc., Vol. 24, No. 8, 1237-1245, 2013.
Printed in Brazil - ©2013 Sociedade Brasileira de Química
0103 - 5053 $6.00+0.00

Article

Nano-Assembled Supramolecular Films from Chitosan-Stabilized Gold Nanoparticles and Cobalt(II) Phthalocyanine

Anna T. B. Silva,[a] Andreane G. Coelho,[a] Lourdes C. da S. Lopes,[a] Marccus V. A. Martins,[b] Frank N. Crespilho,[c] Arben Merkoçi[d] and Welter C. da Silva*,[a]

[a]*Departamento de Química, Centro de Ciências da Natureza, Universidade Federal do Piauí, 64049-550 Teresina-PI, Brazil*

[b]*Centro de Ciências Naturais e Humanas, Universidade Federal do ABC, 09210-170 Santo André-SP, Brazil*

[c]*Departamento de Físico-Química, Instituto de Química de São Carlos, Universidade de São Paulo, 13560-970 São Carlos-SP, Brazil*

[d]*ICN-Institut Catala de Nanociencia i Nanotecnologia, Universitat Autònoma de Barcelona, 08193 Barcelona, Catalonia, Spain*

Neste trabalho, a síntese e a caracterização de nanopartículas de ouro (AuNPs) estabilizadas com quitosana (Chit), assim como a capacidade deste material para formar filmes automontados multicamadas com ftalocianina tetrassulfonada de cobalto(II) (CoTsPc), são reportadas. Este novo material híbrido baseado em Chit-AuNPs e CoTsPc foi caracterizado por diversas técnicas, e as propriedades eletroquímicas de um eletrodo de ITO (óxido de estanho dopado com índio) modificado com Chit-AuNPs e CoTsPc foram investigadas. A quitosana evitou a aglomeração das AuNPs (diâmetro de 6,0 nm), formando uma suspensão coloidal estável por meses. A interação entre as AuNPs e as moléculas de quitosana ocorre principalmente pelos grupamentos CH_2 e NH_3^+ da quitosana. Para os filmes automontados de Chit-AuNPs/CoTsPc, observou-se uma interação supramolecular entre as multicamadas, além do fato de que as AuNPs influenciaram as propriedades redox da CoTsPc. A presença das nanopartículas não só aumentou a área eletroativa do eletrodo, mas também a velocidade de transferência de carga, indicando que este material é um candidato muito promissor para futuras aplicações em dispositivos eletroquímicos.

In this work, we report the synthesis and characterization of gold nanoparticles (AuNPs) stabilized with chitosan (Chit), as well as the capability of this material to form multilayer films with cobalt(II) tetrasulfonated phthalocyanine (CoTsPc). The new hybrid material based on Chit-AuNPs and CoTsPc was characterized by several techniques, and the electrochemical properties of an ITO (indium tin oxide) electrode modified with Chit-AuNPs and CoTsPc were investigated. Chit prevented AuNPs (diameter of 6.0 nm) agglomeration, forming a colloidal suspension that was stable for months. The interaction between the AuNPs and Chit molecules occurs mainly through the CH_2 and NH_3^+ groups from Chit. Supramolecular interaction was observed for multilayer films of Chit-AuNPs/CoTsPc, and the AuNPs influenced the redox properties of CoTsPc. The presence of the nanoparticles not only increased the electroactive area of the electrodes, but also the rate of charge-transfer, suggesting that this material is a very promising candidate for further applications in electrochemical devices.

Keywords: gold nanoparticles, chitosan, supramolecular, layer-by-layer films

*e-mail: welter@ufpi.edu.br

Introduction

There is no doubt that nanomaterials (e.g., biopolymers, metallic nanoparticles, carbon nanotubes, quantum dots, inorganic complexes and others)[1-3] have attracted attention from various fields of science and generated an impact on the technology industry due to the possibility of developing new robust products with unique properties.[1,4] Among the various classes of nanomaterials, hybrid nanomaterials (with organic and inorganic components) can show complex structures at nanoscale, in which the components can interact through hydrophobic force, hydrogen bonding, electrostatic, charge transfer and metal-ligand interaction.[3,5,6] Based on the IUPAC definitions, the term "hybrid" is attributed to a material composed of an intimate mixture of inorganic, organic or both types of components, in which they usually interpenetrate on scales of less than 1 μm.[7] The application of these materials ranges from devices for catalysis in organic reactions[8] to biodevices containing bacteria for use in biosensing.[9]

In recent years, our group showed the possibility of hybrid materials composed by metallophthalocyanines, nanostructures and polyelectrolytes to build blocks with different architectures that allow various applications, such as in electrocatalysis, biosensors, photocatalysis and electrochromic devices.[10-12] The synthetic strategies explore the interactions between metallophthalocyanines and nanostructures in the self-assembly way. As a consequence of the multilayer growth comprising metallophthalocyanines and nanostructures, a refinement of the chemical and physical properties is possible. For these purposes, generally multilayer platforms based on the layer-by-layer (LbL) technique are utilized.[13,14]

LbL is an interesting technique to produce hybrid materials because it is cheap, robust and versatile. Furthermore, LbL is based on the bottom-up approach, from which several types of 2D hybrid material films can be assembled.[11,13] For instance, cobalt(II) tetrasulfonated phthalocyanine (CoTsPc), single-walled carbon nanotubes (SWCNTs) and chitosan (Chit) were used to construct two different platforms (Chit-SWCNTs/CoTsPc and Chit/CoTsPc) aiming at investigating a possible intimate contact between SWCNTs and CoTsPc at the nanoscale level. An evidence of constitutional dynamic chemistry (CDC) concepts was observed in the above mentioned materials. Based on a report by Lehn[15], CDC involves dynamic issues as molecular recognition, reversible interactions and self-organization.

In the present work, a hybrid material based on gold nanoparticles (AuNPs) stabilized by Chit was prepared, and the supramolecular properties of Chit-AuNPs within an LbL film with CoTsPc were investigated. For this purpose, spectroscopic, microscopic and electrochemical techniques were used to investigate the chemical and physical properties of the film. Hybrid materials based on AuNPs have proved to be useful in biocatalytic processes,[10] clinical practice[16] and diagnosis of diseases[17] due to their electroactivity and their electronic and molecular-recognition properties.[18-20] In order to achieve a functional material, Chit was used as a polymeric matrix for film fabrication.[21] The electrochemical properties of the Chit-AuNPs within an LbL film with CoTsPc were also investigated.

Experimental

Chemical and materials

Acetic acid (HAc) was obtained from Vetec. Commercial chitosan (deacetylation degree of 85%) was acquired from Technological Development Park (Ceará State, Brazil) and used in the preparation of 0.5 g L^{-1} chitosan solution utilizing 1.0% HAc (pH 4.0). Chitosan is a copolymer of glucosamine and *N*-acetylglucosamine showing deacetylated structure[22] with primary amine groups available for interactions, also allowing the production of thin films.[11,23] Besides, chitosan has been widely noticed for biomedical and pharmaceutical applications due to its well-known nontoxicity, biocompatibility, biodegradability and hydrating properties.[22] Sodium dihydrogen phosphate (NaH_2PO_4) and sodium monohydrogen phosphate (Na_2HPO_4) were purchased from Dinâmica and Anidrol, respectively, and used to prepare 0.1 mol L^{-1} phosphate buffer solution (PBS, NaH_2PO_4/Na_2HPO_4, pH 7.2). Sodium borohydride ($NaBH_4$) and tetrachloroauric acid trihydrate ($HAuCl_4 \cdot 3H_2O$) were obtained from Aldrich. Chit, $NaBH_4$ and $HAuCl_4 \cdot 3H_2O$ were used in the syntheses of AuNPs. Cobalt(II) tetrasulfonated phthalocyanine was purchased from Porphyrin Systems and utilized without further purification. The CoTsPc and Chit (or Chit-AuNPs) materials were utilized to prepare solutions with concentration of ca. 0.5 g L^{-1} in 1.0% HAc (pH 4.0) and used as polyelectrolyte for LbL fabrication. All other solutions were prepared with water purified by a Purelab Option-Q (Elga) system, with a resistivity of 18.2 MΩ cm.

Synthesis of AuNPs stabilized in chitosan

A solution of $HAuCl_4$ (1.3×10^{-2} mol L^{-1}, 2 mL) was added to 10 mL of a chitosan solution (1.0%) and kept stirring for 3 min. This mixture was then added dropwise to

10 mL of 8.0×10^{-2} mol L^{-1} $NaBH_4$ kept at 0 °C to promote the reduction of Au^{3+} to Au^0, during which a change of solution coloration from yellow to red indicating the formation of AuNPs was observed.[10,17] The product was kept stirring for 3 h. The formation of AuNPs immobilized within the chitosan matrix (Chit-AuNPs) was evidenced by the appearance of the plasmon absorption band at 520 nm.[10,20] For the transmission electronic microscopy (TEM JEOL JEM 2011, 200 kV), a drop of Chit-AuNP suspension was deposited over a copper grid, which it was then air dried. TEM images were obtained digitally by using the Gatan digital micrograph software package. Scheme 1 illustrates the Chit-AuNPs synthesis.

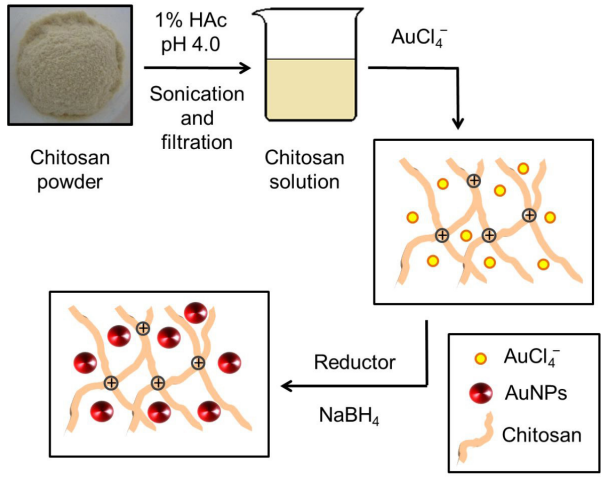

Scheme 1. Schematic representation of the nanocomposite preparation.

In order to investigate the interaction between chitosan molecules and AuNPs, Fourier transform infrared spectroscopic (FTIR) technique was utilized. The experiments were carried out with a Varian 610 IR micro-spectrophotometer. The measurements were performed in the reflectance mode from 4000 to 700 cm^{-1}. The samples (Chit solution and Chit-AuNPs suspension) were deposited on a gold substrate by drop coating and dried in vacuum.

Chit-AuNPs in the form of nanostructured films with CoTsPc multilayers

Self-assembled films were prepared by the LbL method onto ITO (indium tin oxide) and glass substrates using Chit-AuNPs (cationic suspension) and CoTsPc (anionic solution), respectively. For this purpose, the solid substrate was immersed in the Chit-AuNPs suspension for 5 min and washed with acetic acid (pH 4.0) and dried with N_2 gas flow. After Chit-AuNPs layer formation, the substrate was immersed into the CoTsPc solution for 5 min, washed in HAc and dried with N_2 gas. In this step, the first bilayer ITO-{Chit-AuNPs/CoTsPc} was formed. With continuous repetition of this process, the deposition of the desired number of bilayers occurs.[14]

UV-Vis spectra (using a double beam Hitachi U-3000 spectrophotometer) of the Chit, Chit-AuNPs and CoTsPc samples were registered before and after the production of cast films immobilized on quartz substrate and dried in a desiccator. Also, the electronic spectra in the visible region of Chit-AuNPs/CoTsPc using hydrophilic glass substrates (recorded after each deposition step utilizing 1 to 10 bilayers) were obtained. For AFM study, glass plates coated with gold film were used as substrates for deposition of the materials. The AFM images were obtained from LbL films containing 1, 3 and 5 bilayers deposited onto ITO electrodes using an Agilent 5500 equipment with cantilevers operating in the intermittent-contact mode (AC mode), slightly below their resonance frequency of approximately 290 kHz. Image processing and the determination of the roughness (RMS) were performed by using Gwyddion software version 2.26.

The electrochemical experiments were carried out using ITO and ITO-modified electrodes. The cast and LbL films were deposited onto ITO electrode and utilized in the cyclic voltammetry (CV) experiments using an Autolab PGSTAT 30 potentiostat. For CV measurements, 5.0×10^{-3} mol L^{-1} potassium ferricyanide, $K_3[Fe(CN)_6]$, in 0.1 mol L^{-1} KCl (scan rate of 0.005 to 0.5 V s^{-1}) was used as electrolyte in order to evaluate the charge transfer kinetics on the Chit-AuNPs-modified electrodes. The electrochemical cell with three electrodes contained: (*i*) ITO or ITO modified electrode (area of 0.24 cm^2) as working electrode, (*ii*) saturated calomel reference (SCE) as reference electrode, and (*iii*) platinum wire as counter electrode. PBS (pH 7.2) electrolyte was also employed as supporting electrolyte. Prior to the electrochemical experiments, oxygen was removed from the electrolyte by bubbling N_2 gas (99.9%) through the electrochemical cell for 15 min.

Results and Discussion

Synthesis and characterization of Chit-AuNPs

The synthesis of AuNPs was first confirmed by electronic spectroscopy (UV-Vis), in which the presence of a plasmonic band at 520 nm (Figure 1) attributed to AuNPs was observed.[10,17,20] It is well-known that nanomaterials exposed to light also promote the scattering. Thereby, the total light absorbance is a contribution of absorbed radiation (α_{abs}) and of scattered radiation (α_{sca}), thus plasmon absorption band depends on size, shape,

aggregation and spatial distribution of NPs.[24,25] It was observed that AuNPs were stabilized by chitosan and the Chit-AuNPs suspension showed a higher extinction than solid-phase Chit-AuNPs (immobilized onto glass substrate). This fact can be related to a higher concentration of nanoparticles dispersed in water than onto the quartz surface. Regarding the plasmon energy, the literature reports[1,25] that the increase in particle size or self-organization of NPs into clusters in cast films causes bathochromic effect. The latter is observed for the Chit-AuNPs nanocomposite as a shift from 520 to 525 nm when the AuNPs are immobilized on the solid surface.

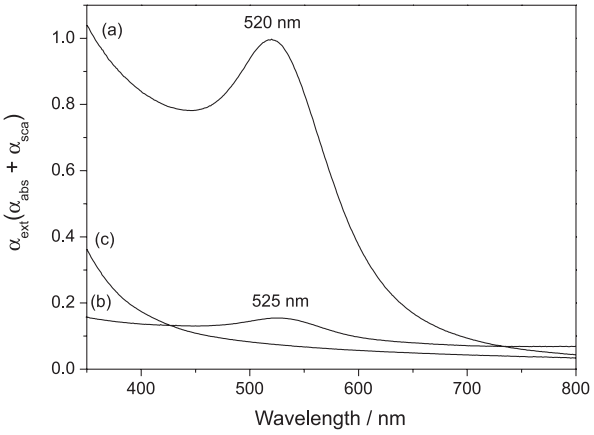

Figure 1. Electronic spectra in the visible region for: (a) Chit-AuNPs in aqueous suspension, (b) Chit-AuNPs immobilized onto a quartz substrate and (c) Chit solution.

The AuNPs stabilization by the Chit molecules was also investigated by FTIR spectroscopy in the reflectance mode. Generally, FTIR spectra for Chit and Chit-AuNPs (Figure 2) show slight differences. For both spectra, a broad characteristic band in the 3100-3550 cm^{-1} region, attributed to O–H stretching, which normally overlaps the N–H stretching was observed.[26] However, the symmetrical and anti-symmetrical C–H stretchings in the 2900-2500 cm^{-1} region present in the Chit spectrum practically disappear after immobilization of the AuNPs. This effect can also be associated to changes in the symmetry of the $–CH_n$ group. The peaks centered at 1650 and 1575 cm^{-1} in the Chit spectrum were assigned to C=O stretching (amide group CONHR) and N–H stretching (protonated amino peak), respectively. The cited peaks are related to the degree of *N*-deacetylation of chitin.[26,27] The ν_{NH} peak shift to low energy is observed in the Chit-AuNPs spectrum, even at half the concentration of $HAuCl_4$ reported in Chit-AuNPs synthesis, probably due to the interaction between the AuNPs and Chit polymer (zoomed region, Figure 2B).[26] These results are consistent with those reported by Huang *et al.*,[27] who observed a blue-shift of the coupling of $\nu_{C=O}$ and ν_{N-H} for an AuNPs/carboxymethylated chitosan (CM-Chit) nanocomposite, and they proposed two reasons for changes in the spectrum. First, the electrostatic repulsive interaction between AuNPs and CM-Chit occurs, and second, the formation of coordination bonds between AuNPs and nitrogen/oxygen atoms of carboxymethylated chitosan is speculated. Additionally, the asymmetrical C–H bending (CH_2 group), oxy bridge stretching (C–O–C from glucosamine unit) and C–O skeletal stretching at 1420, 1065 and 1012 cm^{-1}, respectively, decrease in relative intensity for Chit-AuNPs spectrum. Based on all these results, a possible intimate contact between Chit (mainly through of CH_2 and NH_3^+ groups) and AuNPs, as suggested in Scheme 2, may have occurred.

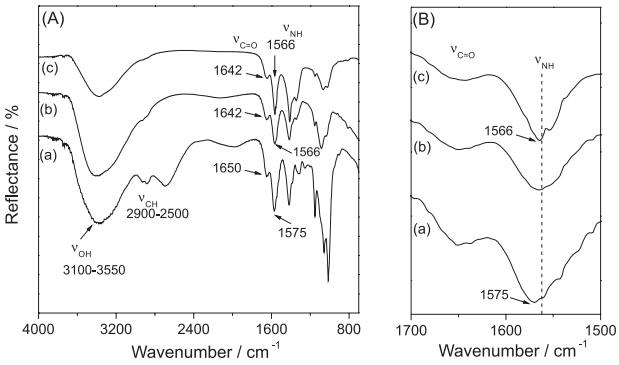

Figure 2. (A) FTIR spectra (reflectance mode) for: (a) chitosan, (b) diluted Chit-AuNPs and (c) Chit-AuNPs; (B) zoomed region of the N–H stretching.

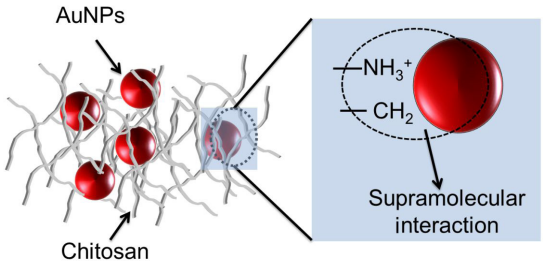

Scheme 2. Schematic representation of the molecular interaction between chitosan and AuNPs.

Aiming at evaluating the size, distribution and structure of AuNPs, the Chit-AuNPs suspension was deposited onto a copper grid and analyzed by TEM. As observed in Figure 3, the AuNPs exhibited spherical shape. The size distribution histogram for AuNPs revealed a mean diameter of 6.0 nm (n = 421 nanoparticles). This distribution and the absence of agglomerates suggest that the Chit matrix prevents the agglomeration of AuNPs. Furthermore, Chit interacts effectively with AuNPs avoiding both uncontrollable nucleation of AuNPs and their aggregation.[28] It is important

to mention that Chit-AuNPs showed excellent stability in aqueous suspension over 3 months, during which the λ_{max} of the plasmonic band remained the same. Other authors have also proposed several mechanisms to explain the AuNP stabilization[28,29] in organic matrices. For instance, Brunel *et al.*[29] showed the influence of several parameters associated with the AuNP stabilization, such as time, ionic strength, temperature and pH. The authors proposed three stabilization mechanisms: (*i*) electrostatic and steric stabilization, achieved as function of acid pH and low ionic strength; (*ii*) steric stabilization only, that depends on both acid pH and high ionic strength; and (*iii*) no stabilization, generally evidenced at neutral pH. In the case of our results, since the Chit-AuNP suspension showed low pH (4.80) and high ionic strength, the second mechanism above mentioned,[29] with formation of $R–NH_3^+$ group from chitosan, is more favorable. It is also reasonable to point to the formation of a tridimensional net involving chitosan and AuNPs since CH_2 groups are also affected by the presence of nanoparticles. Although it is not possible to conclude from these results what are the real contributions of each of these chemical groups to the effective interaction with AuNPs, different molecular interactions based on different kinds of binding contributing to nanoparticle stabilization are almost evident.[5]

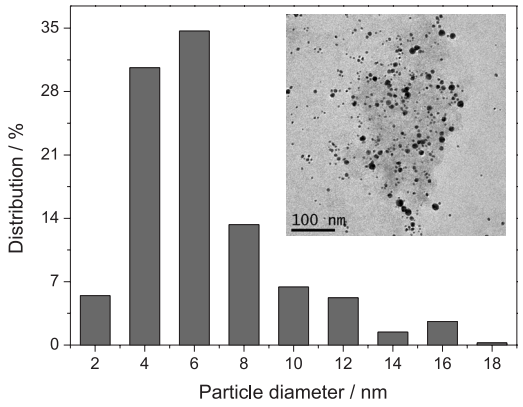

Figure 3. Histograms of the AuNP diameters obtained from TEM images (421 nanoparticles), showing size distributions of the AuNPs protected by the Chit polymer.

Electrochemical properties of cast films based on Chit and Chit-AuNPs

In order to investigate the electrochemical properties of Chit-AuNP films looking for future applications in electrochemical devices, cast films based on Chit and Chit-AuNPs were deposited onto ITO electrodes. The idea was to study if AuNPs cause significant changes to the electrochemical properties of the ITO-modified electrodes. For this purpose, two electrodes were prepared: for the first one, 40 μL of chitosan suspension (0.5 g L^{-1}) were deposited onto ITO surface (0.24 cm^2, ITO-Chit), while the second electrode was prepared in a similar way, but with the presence of AuNPs (ITO-Chit-AuNPs), with the same concentration of chitosan. The electrodes were utilized in cyclic voltammetry experiments, in the presence of 5.0×10^{-3} mol L^{-1} hexacyanoferrate (III) (electrolyte 0.1 mol L^{-1} KCl). Figure 4 reports the voltammograms obtained for bare ITO, ITO-Chit and ITO-Chit-AuNPs in the range from −0.8 to 0.8 V (*vs.* SCE). The voltammograms exhibited a well-defined redox pair, with $E_{1/2}$ centered at 0.190 V, assigned to $[Fe^{II}(CN)_6]^{4-}/[Fe^{III}(CN)_6]^{3-}$ conversion. When compared to the bare ITO, the current densities for ITO-Chit showed slight decrease probably due to the insulating properties of chitosan. For ITO-Chit-AuNPs, an increase of approximately 320% on the peak currents is observed.

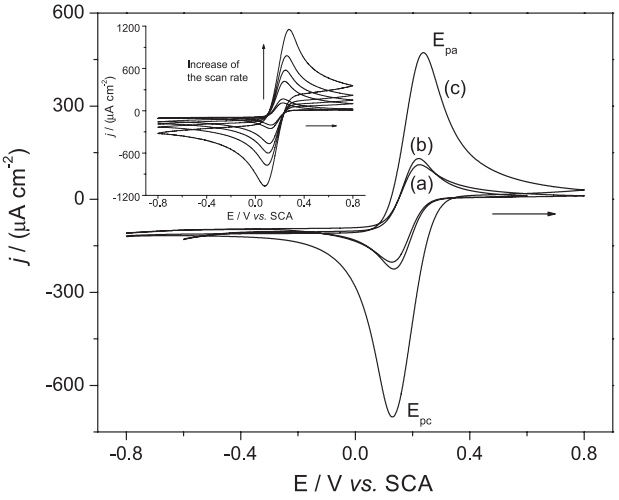

Figure 4. Cyclic voltammograms for the three electrodes: (a) bare ITO, (b) ITO-Chit and (c) ITO-Chit-AuNPs at the scan rate of 0.050 V s^{-1}. Inset: Chit-AuNPs cast film in the rates of 0.005, 0.01, 0.05, 0.1, 0.3 and 0.5 V s^{-1}. Electrolyte: 5.0×10^{-3} mol L^{-1} $K_3[Fe(CN)_6]$ in 0.1 mol L^{-1} KCl solution, T = 25 °C.

Two factors may be contributing to the increase of the current. First, the electroactive area of the electrode increased, and thus the current must increase proportionally. Second, the gold nanoparticles can increase the conductivity of the film, causing less blockage effect when compared with ITO-Chit, leading to more species that react effectively at interface. Probably, the effect of the electroactivity area is more prominent. As also supported by AFM experiments (discussed in sequence), there is an increase in average roughness when there are AuNPs on the electrode surface. Although the electroactive area of the electrode increases, AuNPs also play an important role in the electron transfer. This can be verified when calculating the rate constant for electron transfer (k_{ET}).

The literature has reported several electrochemical techniques for determining k_{ET} in redox-active molecules, such as cyclic voltammetry (CV), chronoamperometry (CA), alternating current voltammetry (ACV) and electrochemical impedance spectroscopy (EIS).[30,31] All these approaches show some advantages and disadvantages. In this work, the sweep method from CV was employed, since the idea was just to compare k_{ET} for ITO, ITO-Chit and ITO-Chit-AuNP electrodes. The Laviron method was applied,[32] which is a mathematical treatment based on the Butler-Volmer formalism. It is worth mentioning that, for others systems (e.g., enzyme modified electrodes), more accurate values of k_{ET} are obtained by using Marcus theory.[31,33-36] As observed in Figures 5a and 5c, the ITO-Chit-AuNPs electrode revealed a linear plot for both cathodic and anodic peak currents for the $[Fe^{II}(CN)_6]^{4-}/[Fe^{III}(CN)_6]^{3-}$ pair against the scan rate, indicating diffusion controlled process. The logarithm of the square root of scan rate *vs.* peak potential is shown in Figure 5b, in which an increase in the scan rate resulted in a shift of the oxidation wave to a more positive potential, while the reduction wave shifted to a more negative potential. For the latter, a plot of $E_p = f(\log \nu)$ yielded two straight lines corresponding to a slope $-\beta RT/\alpha nF$ for the cathodic peak and $\beta RT/(1-\alpha)nF$ for the anodic peak, where β is constant. Based on the slope of the straight lines, the charge transfer coefficient (α) determined was 0.08. Thus, based on the Laviron formalism, k_{ET} for electron transfer between the ITO-Chit-AuNPs electrode and the $[Fe^{II}(CN)_6]^{4-}/[Fe^{III}(CN)_6]^{3-}$ redox pair was also of 1.50 s^{-1}. The same approach was also employed for ITO and ITO-Chit electrodes in the same experimental conditions as for ITO-Chit-AuNPs, leading to values of k_{ET} for electron transfer of 0.90 and 0.61 s^{-1}, respectively (Figures S1 and S2 in the Supplementary Information (SI) section). The $k_{ET(ITO)} > k_{ET(ITO\text{-}Chit)}$ result means that the chitosan polymer can partially hinder the electron transfer. On the other hand, $k_{ET(ITO\text{-}Chit\text{-}AuNPs)} > k_{ET(ITO)} > k_{ET(ITO\text{-}Chit)}$ provided a strong indication that not only the geometrical area of the electrode contributes to enhance the faradaic currents, but also the presence of AuNPs contributes to increase the rate of heterogeneous charge-transfer at the interface.

The processing of Chit-AuNPs in the form of nanostructured films with CoTsPc multilayers

In order to apply Chit-AuNPs in the preparation of nanostructured films, CoTsPc and Chit-AuNPs were assembled alternately onto solid substrates by LbL. Cobalt(II) phthalocyanine was chosen because it is a material with many potential applications ranging from photovoltaic devices to biosensors applied in diagnostics.[17] Thus, multilayers comprising Chit-AuNPs and CoTsPc were assembled onto different solid substrates (glass, ITO and glass covered with gold). Films from 1 to 10 bilayers of Chit-AuNPs/CoTsPc were characterized by electronic spectroscopy, cyclic voltammetry and AFM.

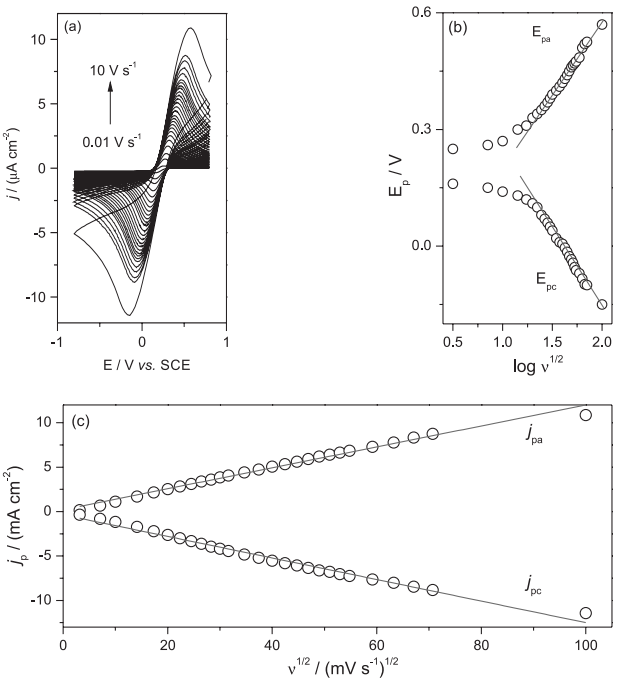

Figure 5. (a) Cyclic voltammograms of ITO-Chit-AuNPs with increasing scan rate from 0.01 to 10 V s^{-1}. (b) Variation of peak potential (E_{pa} and E_{pc}) *vs.* logarithm of $\nu^{1/2}$ for ITO-Chit-AuNPs. (c) Plot of the cathodic (j_{pc}) and anodic (j_{pa}) peak currents *vs.* $\nu^{1/2}$. Electrolyte: 5.0×10^{-3} mol L^{-1} $K_3[Fe(CN)_6]$ in 0.1 mol L^{-1} KCl solution, T = 25 °C.

The UV-Vis spectra of metallic phthalocyanines are typically dominated by two strong absorptions called B (or Soret) and Q bands. The B band is attributed to the ligand transition and the Q band is composed of the two strong absorptions due to the formation of monomeric and dimeric species.[37] For LbL films, as observed in Figure 6, the UV-Vis spectra for $\{$Chit-AuNPs/CoTsPc$\}_n$ exhibited two main absorptions for CoTsPc compound at 334 and 613 nm, assigned to the macrocycle ligand (B band) and dimeric species, respectively. Also, a prominent shoulder at 681 nm is attributed to the monomeric CoTsPc species, which normally increases in intensity for CoTsPc in solution. The plasmonic band (at 520 nm) previously observed for Chit-AuNPs in aqueous suspension was not observed for the LbL film. This band was overlapped by the Q band (CoTsPc), which exhibits a higher extinction coefficient.[10] Similar behavior was observed in other studies related to the immobilization of metallic nanoparticles within thin films.[9,22] The electronic spectra of the Chit-AuNPs and CoTsPc species (Figure S3 in the SI section) show a

comparison between the spectra for the cast film of Chit-AuNPs and CoTsPc.

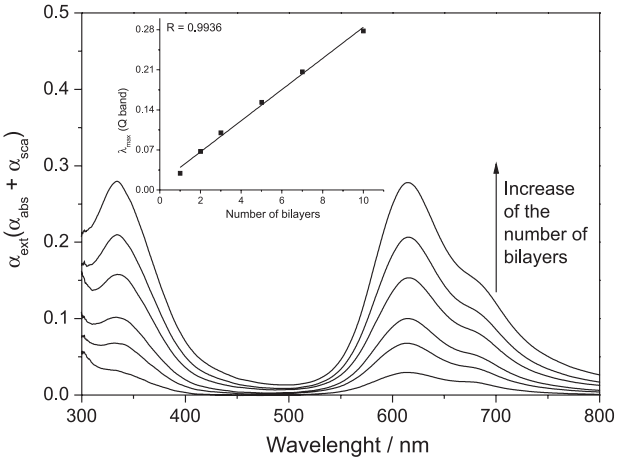

Figure 6. Electronic spectra showing the growth of the {Chit-AuNPs/CoTsPc}$_n$ system, with n = number of bilayers (from 1 to 10). Inset: λ_{max} (Q band) *vs.* number of bilayers.

The Q band from CoTsPc was utilized to confirm the growth of Chit-AuNPs/CoTsPc multilayers, from 1 to 10 bilayers. As observed in Figure 6, the intensity of the Q band (λ_{max} at 613 nm) increases linearly with bilayers numbers, indicating that the same amount of CoTsPc was incorporated in each LbL deposition. The linear growth was confirmed by plotting of λ_{max} of the Q band *vs.* the number of bilayers, which showed good linearity (R = 0.9936). Similar behavior was observed for LbL systems produced from Chit-SWNTC, PAH, PAH-AuNPs, NiTsPc and CoTsPc: {PAH/CoTsPc},[12] {PAH/NiTsPc},[10] {PAH-AuNPs/NiTsPc}[10] and {Chit-SWCNT/CoTsPc}.[11] The stability of multilayer deposition for metallophthalocyanine and (bio)polymer species has been interpreted as arising from the strong electrostatic interactions between oppositely charged materials that occur at supramolecular level.[38] However, hydrophobic and hydrogen interactions can also play a fundamental role in the stabilization of polymers and complex compounds in LbL films.[1,2,10] The supramolecular organization of CoTsPc and chitosan is confirmed in LbL films estimating the ratio between the absorption intensities of dimeric and monomeric species (I_{dim}/I_{mon}).[11] The {Chit-AuNPs/CoTsPc} system with one bilayer had a I_{613}/I_{681} of 1.78, then it reaches values of 1.93 for 2 and 3-bilayers. With a 5-bilayer LbL film, the I_{613}/I_{681} relation decreases to 1.86, which practically does not change until formation of 10 bilayers (Table S1 in the SI section). Thus, this result indicates that the amount of H-aggregates with dimer formation within LbL films decreases after new multilayer deposition. It is interesting to mention that the I_{613}/I_{668} relation for CoTsPc species in solution was 1.52. This value is lower than the observed for the LbL system, indicating that the CoTsPc-CoTsPc molecular interaction for dimer formation in solution is less pronounced.

AFM images of the {Chit/CoTsPc} and {Chit-AuNPs/CoTsPc} platforms containing 1, 3 and 5 bilayers, generated under an area of 1.0 × 1.0 μm^2 are shown in Figure 7. The topographical analysis for all modified electrodes showed a globular morphology with increase of both average roughness (R_{ms}) values after new bilayer depositions. Comparing the R_{ms} values for the mentioned systems, it is evident that AuNP incorporation within LbL films caused an increase in roughness in comparison to those observed for the {Chit/CoTsPc} system (Table S2 in the SI section). Differently from {Chit-SWCNT/CoTsPc}$_5$,[11] the {Chit-AuNPs/CoTsPc}$_5$ modified electrode (containing AuNPs) exhibited a lower roughness probably due to the fact that the Chit-AuNPs nanocomposite favors high packing of monolayers in the 2D structures. Besides, an interpenetration of adjacent layers for LBL containing nanotubes and chitosan is expected.

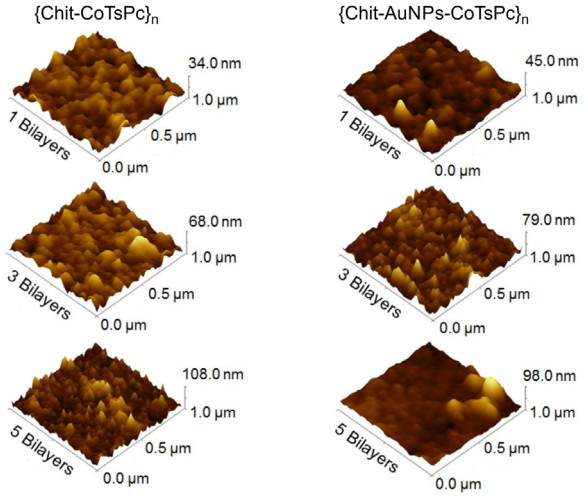

Figure 7. AFM images for the {Chit/CoTsPc}$_n$ and {Chit-AuNPs/CoTsPc}$_n$ systems containing 1, 3 and 5 bilayers deposited onto ITO substrate.

Cyclic voltammetry was utilized to investigate both electrochemical properties and growth of the {Chit-AuNPs/CoTsPc}$_n$ LbL films. Voltammograms for LbL films with 1, 3, 7 and 10 bilayers on ITO (geometric area of 0.24 cm^2) showed a linear increase of the peak current with the number of bilayers (Figure S4 in the SI section). This result is in agreement with UV-Vis results. Figure 8 shows the cyclic voltammograms for bare ITO and ITO-{Chit-AuNPs/CoTsPc}$_3$. The ITO-{Chit-AuNPs/CoTsPc}$_3$ modified electrodes showed a redox process at –0.60 V (*vs.* SCE) attributed to the $[Co^{I}TsPc]^{5-}/[Co^{II}TsPc]^{4-}$ couple and an irreversible process at 0.70 V (E_{pa2}) assigned to conversion of $Co^{II}TsPc$ to $Co^{III}TsPc$ species.[12]

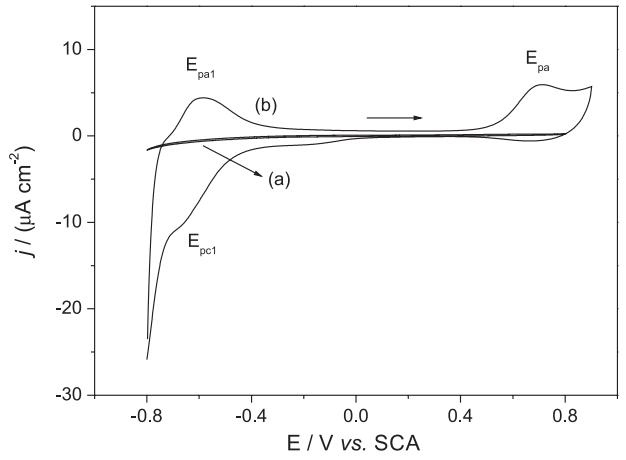

Figure 8. Cyclic voltammograms for the (a) bare ITO and (b) ITO-{Chit-AuNPs/CoTsPc}$_3$. Electrolyte: 0.1 mol L^{-1} PBS (pH 7.2), scan rate of 0.5 V s^{-1}.

As expected, 3-bilayer LbL film assembled with Chit and polystyrenesulfonic acid (PSS) (without Co^{II}TsPc) did not exhibit electrochemical processes from –0.8 to 0.9 V since the PSS polymer is not electroactive (Figure S6 in the SI section). The charge transfer within the multilayers film was analyzed through the influence of the scan rate (0.01 to 0.5 V s^{-1} range) on the oxidation and reduction current peaks of CoTsPc (Figure S6 in the SI section). The results showed a good linearity for the plot of current density *vs.* scan rate, indicating that the electrochemical reaction is limited by the charge transfer along multilayers. Furthermore, AuNPs enhance the charge transfer within multilayers containing CoTsPc and Chit molecules. For instance, k_{ET} for ITO-{Chit/CoTsPc}$_3$ and ITO-{Chit-AuNPs/CoTsPc}$_3$ was obtained (Figure S7 and Table S3 in the SI section). Despite the immobilization of an insulating material (chitosan), the incorporation of AuNPs in LbL film clearly causes an increase in k_{ET} from 0.30 to 0.93 s^{-1}. Also, the ITO-{Chit-AuNPs/CoTsPc}$_3$ electrode is very stable, when the faradaic current remains stable up to 20 cycles using a scan rate of 0.1 V s^{-1} in 0.1 mol L^{-1} PBS solution (pH 7.2) (Figure S8 in the SI section). The faradaic currents practically do not change, even after long storage time (2 months), suggesting high chemical and electrochemical stability.

Conclusions

This work focused on the preparation and characterization of AuNPs stabilized into a Chit matrix as well as their immobilization with CoTsPc to form LbL films. A new hybrid material based on Chit-AuNPs and CoTsPc was characterized by several techniques, and the electrochemical properties of ITO-modified electrode with Chit-AuNPs and CoTsPc were investigated. The main findings of this study can be described as follows.

By using the experimental conditions described here, AuNPs with spherical morphology can be obtained in the presence of the Chit biopolymer. Chit molecules prevented the AuNP agglomeration, as evidenced by TEM images. AuNPs are stabilized with chitosan in aqueous suspension for months. The molecular interaction between AuNPs and Chit molecules can occur mainly through CH_2 and NH_3^+ groups from Chit, as observed from FTIR results. This can explain the well-defined spherical morphology of nanoparticles and also the capability of Chi to prevent the AuNP agglomeration.

ITO electrodes modified with a cast film of Chit-AuNPs can be easily prepared, for instance by dropping the Chit-AuNPs suspension on the electrode surface. Cyclic voltammograms revealed that there is an increase in the faradaic currents of the $[Fe^{II}(CN)_6]^{4-}/[Fe^{III}(CN)_6]^{3-}$ reaction on ITO-Chit-AuNPs surface when compared with currents obtained by using bare-ITO and ITO-Chit electrodes. Probably, the increase of the electroactivity area is very representative, since the AFM experiments indicated that AuNPs increase the electrode roughness. On the other hand, k_{ET} obtained for ITO-Chit-AuNPs electrode showed that the AuNPs increase the rate of charge-transfer.

Finally, CoTsPc and Chit-AuNPs were successfully immobilized as multilayered films on different solid substrates. From electronic spectroscopy results, supramolecular organization of CoTsPc and chitosan is observed in LbL films. By estimating the ratio between the absorption intensities of dimeric and monomeric species (I_{dim}/I_{mon}), it was observed that the amount of H-aggregates with dimer formation within LbL films decreases after new multilayer deposition. However, dimer formation in solution is less pronounced than in the LbL films. The supramolecular organization of Chit-AuNPs and CoTsPc in a multilayer way permitted the build-up of highly stable ITO-{Chit-AuNPs/CoTsPc}$_3$ electrodes. Furthermore, AuNPs in LbL film promoted an increase on the charge-transfer rate, suggesting that this kind of electrode is a very promising candidate for further application in electrochemical devices.

Supplementary Information

Supplementary information is available free of charge at http://jbcs.sbq.org.br as a PDF file.

Acknowledgements

The authors acknowledge the financial support from FAPEPI, CNPq (472369/2008-3 and 577410/2008-3

projects), FAPESP (project number 2011/01541-0), CAPES (nBioNet) and MEC (Spain) for MAT2011-25870 project.

References

1. Grzelczak, M.; Vermant, J.; Furst, E. M.; Liz-Marzán, L. M.; *ACS Nano* **2010**, *4*, 3591.
2. Ariga, K.; Ishihara, S.; Abe, H.; Li, M.; Hill, J. P.; *J. Mater. Chem.* **2012**, *22*, 2369; Ariga, K.; Hill, J. P.; Lee, M. V.; Vinu, A.; Charvet, R.; Acharya, S.; *Sci. Technol. Adv. Mater.* **2008**, *9*, 1.
3. Silva, A. T. B.; Magalhães, J. L.; Sousa, E. H. S.; Silva, W. C. In *Nanobioelectrochemistry*; Crespilho, F. N., ed.; Springer: Berlin, Germany, 2012, ch. 5.
4. Winkler, P. M.; Steiner, G.; Vrtala, A.; Vehkamäki, H.; Noppel, M.; Lehtinen, K. E. J.; Reischl, G. P.; Wagner, P. E.; Kulmala, M.; *Science* **2008**, *319*, 1374.
5. Walker, D. A.; Kowalczyk, B.; Cruz, M. O.; Grzybowski, B. A.; *Nanoscale* **2011**, *3*, 1316.
6. Yoon, H.; Jang, W.; *J. Mater Chem.* **2010**, *20*, 211; Kotov, N. A.; *Nanostruct. Mater.* **1999**, *12*, 789.
7. McNaught, A. D.; Wilkinson, A.; *Compendium of Chemical Terminology*, 2nd ed.; Blackwell Scientific Publications: Oxford, UK, 1997.
8. Li, H.; Han, L.; Cooper-White, J.; Kim, I.; *Green Chem.* **2012**, *14*, 586.
9. Sefcovicová, J.; Filip, J.; Gemeiner, P.; Vikartovská, A.; Pätoprstý, V.; Tkac, J.; *Electrochem. Commun.* **2011**, *13*, 966.
10. Alencar, W. S.; Crespilho, F. N.; Martins, M. V. A.; Zucolotto, V.; Oliveira Jr., O. N.; Silva, W. C.; *Phys. Chem. Chem. Phys.* **2009**, *11*, 5086.
11. Luz, R. A. S.; Martins, M. V. A.; Magalhães, J. L.; Siqueira Jr., J. R.; Zucolotto, V.; Oliveira Jr., O. N.; Crespilho, F. N.; Silva, W. C.; *Mater. Chem. Phys.* **2011**, *130*, 1072.
12. Santos, A. C.; Luz, R. A. S.; Ferreira, L. G. F.; Santos Jr., J. R.; Silva, W. C.; Crespilho, F. N.; *Quim. Nova* **2010**, *33*, 539
13. Silva, W. C.; Guix, M.; Angeles, G. A.; Merkoçi, A.; *Phys. Chem. Chem. Phys.* **2010**, *12*, 15505.
14. Decher, G.; *Science* **1997**, *277*, 1232.
15. Lehn, J. M.; *Chem. Soc. Rev.* **2007**, *36*, 151.
16. Thakor, A. S.; Jokerst, J.; Zavaleta, C.; Massoud, T. F.; Gambhir, S. S.; *Nano Lett.* **2011**, *11*, 4029.
17. Escosura-Muñiz, A.; Merkoçi, A.; *Expert Opin. Med. Diagn.* **2010**, *4*, 21.
18. Chegel, V.; Rachkov, O.; Lopatynskyi, A.; Ishihara, S.; Yanchuk, I.; Nemoto, Y.; Hill, J. P.; Ariga, K.; *J. Phys. Chem. C* **2012**, *116*, 2683.
19. Lu, L.; Ai, K.; Ozaki, Y.; *Langmuir* **2008**, *24*, 1058.
20. Romo-Herrera, J. M.; Alvarez-Puebla, R. A.; Liz-Marzán, L. M.; *Nanoscale* **2011**, *3*, 1304.
21. Maity, A. R.; Jana, N. R.; *J. Phys. Chem. C* **2011**, *115*, 137.
22. Gartner, C.; López, B. L.; Sierra, L.; Graf, R.; Spiess, H. W.; Gaborieau, M.; *Biomacromolecules* **2011**, *12*, 1380.
23. Manna, U.; Patil, S.; *J. Phys. Chem. B* **2009**, *113*, 9137.
24. Creighton, J. A.; Eadont, D. G.; *J. Chem. Soc., Faraday Trans.* **1991**, *87*, 3881.
25. Kasthuri, J.; Rajendiran, N.; *Colloids Surf., B* **2009**, *73*, 387.
26. Kumirska, J.; Czerwicka, M.; Kaczyński, Z.; Bychowska, A.; Brzozowski, K.; Thöming, J.; Stepnowski, P.; *Mar. Drugs* **2010**, *8*, 1567.
27. Huang, L.; Zhai, M.; Peng, J.; Xu, L.; Li, J.; Wei, G.; *J. Colloid Interface Sci.* **2007**, *316*, 398.
28. Divsar, F.; Nomani, A.; Chaloosi, M.; Haririan, I.; *Microchim. Acta* **2009**, *165*, 421.
29. Brunel, F.; Véron, L.; Ladavière, C.; David, L.; Domard, A.; Delair, T.; *Langmuir* **2009**, *25*, 8935.
30. Eckermann, A. L.; Feld, D. J.; Shaw, J. A.; Meade, T. J.; *Coord. Chem. Rev.* **2010**, *254*, 1769.
31. Léger, C.; Bertrand, P.; *Chem. Rev.* **2008**, *108*, 2379.
32. Laviron, E.; *J. Electroanal. Chem. Interfacial Electrochem.* **1979**, *101*, 19.
33. Marcus, R. A.; *J. Chem. Phys.* **1956**, *24*, 979.
34. Marcus, R. A.; *J. Chem. Phys.* **1956**, *24*, 966.
35. Marcus, R. A.; *Annu. Rev. Phys. Chem.* **1964**, *15*, 155.
36. Marcus, R. A.; Sutin, N.; *Biochim. Biophys. Acta* **1985**, *811*, 265.
37. Leznoff, C. C.; Lever, A. B. P.; *Phtalocyanines Properties and Applications*, vol. 3; VHC Publishers: New York, USA, 1993.
38. Terzi, F.; Zanardi, C.; Lukkari, J.; Zanfrognini, B.; Pigani, L.; Seeber, R.; Aaritalo, T.; Kankare, J.; *J. Phys. Chem. C* **2009**, *113*, 4868.

Submitted: August 14, 2012
Published online: June 28, 2013

FAPESP has sponsored the publication of this article.

J. Braz. Chem. Soc., Vol. 24, No. 8, S1-S4, 2013.
Printed in Brazil - ©2013 Sociedade Brasileira de Química
0103 - 5053 $6.00+0.00

Supplementary Information

Nano-Assembled Supramolecular Films from Chitosan-Stabilized Gold Nanoparticles and Cobalt(II) Phthalocyanine

Anna T. B. Silva,[a] Andreane G. Coelho,[a] Lourdes C. da S. Lopes,[a] Marccus V. A. Martins,[b] Frank N. Crespilho,[c] Arben Merkoçi[d] and Welter C. da Silva*,[a]

[a]*Departamento de Química, Centro de Ciências da Natureza, Universidade Federal do Piauí, 64049-550 Teresina-PI, Brazil*

[b]*Centro de Ciências Naturais e Humanas, Universidade Federal do ABC, 09210-170 Santo André-SP, Brazil*

[c]*Departamento de Físico-Química, Instituto de Química de São Carlos, Universidade de São Paulo, 13560-970 São Carlos-SP, Brazil*

[d]*ICN-Institut Catala de Nanociencia i Nanotecnologia, Universitat Autònoma de Barcelona, 08193 Barcelona, Catalonia, Spain*

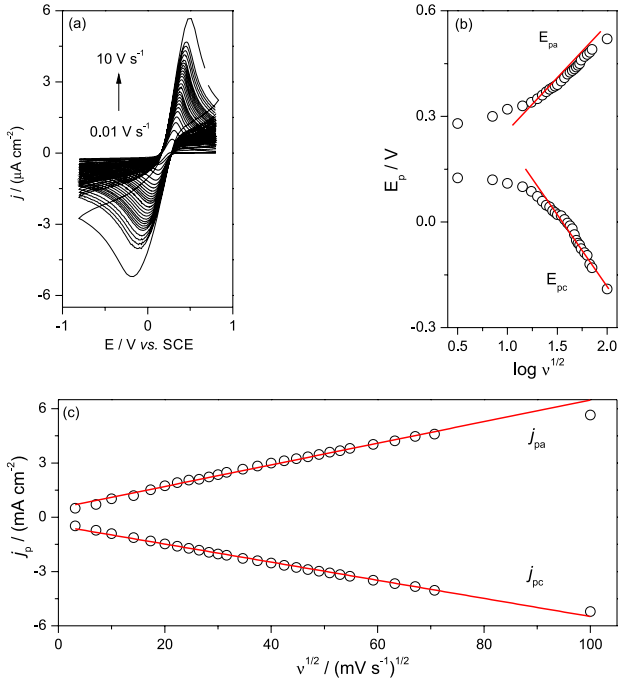

Figure S1. (a) Cyclic voltammograms of bare ITO with increasing scan rate from 0.01 to 10 V s^{-1}. (b) Variation of peak potential (E_{pa} and E_{pc}) *vs.* log $\nu^{1/2}$ of ITO. (c) Plot of the cathodic (j_{pc}) and anodic (j_{pa}) peak currents *vs.* $\nu^{1/2}$. Electrolyte: 5.0 × 10^{-3} mol L^{-1} $K_3[Fe(CN)_6]$ in 0.1 mol L^{-1} KCl solution, T = 25 °C.

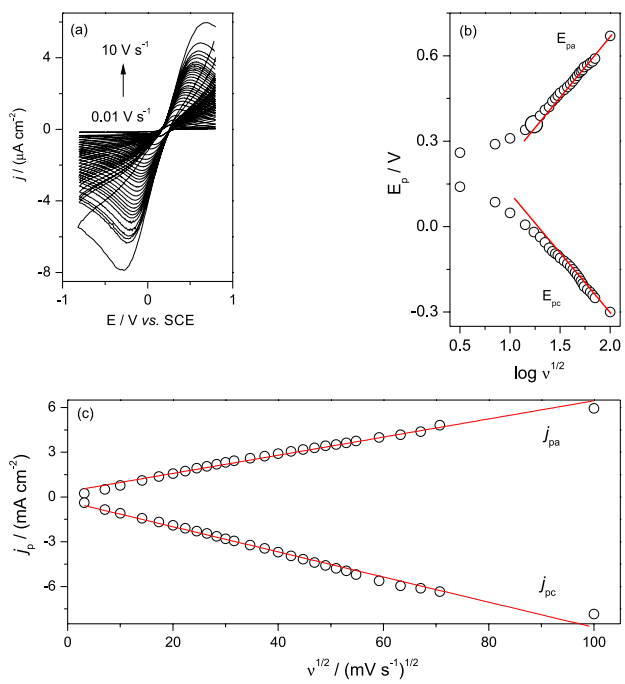

Figure S2. (a) Cyclic voltammograms of the ITO-Chit modified electrode with increasing scan rate from 0.01 to 10 V s^{-1}. (b) Variation of peak potential (E_{pa} and E_{pc}) *vs.* log $\nu^{1/2}$ for ITO-Chit. (c) Plot of the cathodic (j_{pc}) and anodic (j_{pa}) peak currents *vs.* $\nu^{1/2}$. Electrolyte: 5.0 × 10^{-3} mol L^{-1} $K_3[Fe(CN)_6]$ in 0.1 mol L^{-1} KCl solution, T = 25 °C.

*e-mail: welter@ufpi.edu.br

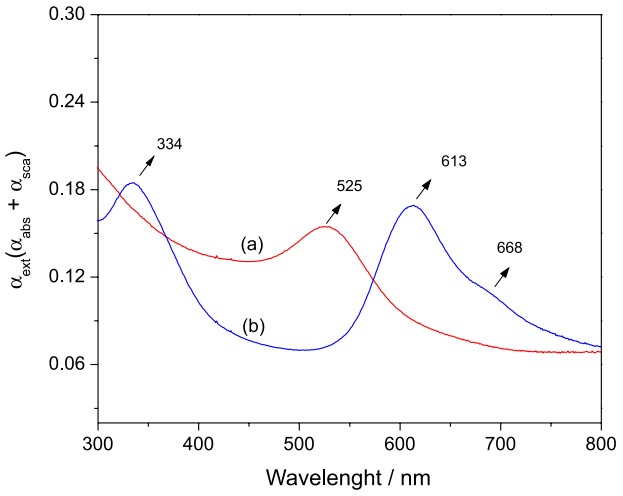

Figure S3. Comparison between the UV-Vis spectra of the cast films: (a) Chit-AuNPs and (b) CoTsPc.

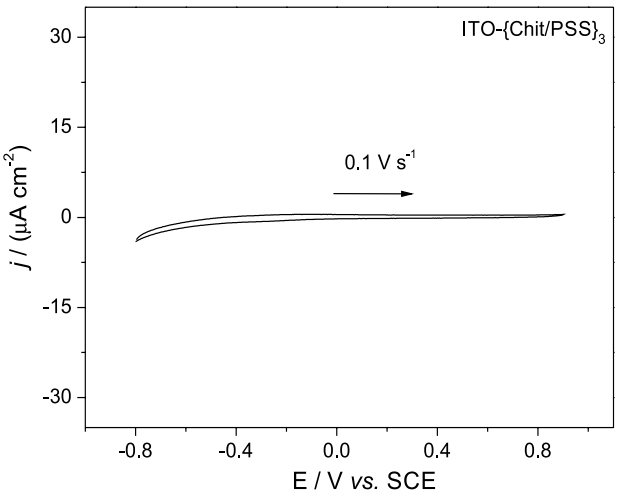

Figure S5. Cyclic voltammogram for the ITO-{Chit/PSS}$_3$ film in 0.1 mol L^{-1} PBS electrolyte (pH 7.2), scan rate of 0.1 V s^{-1}.

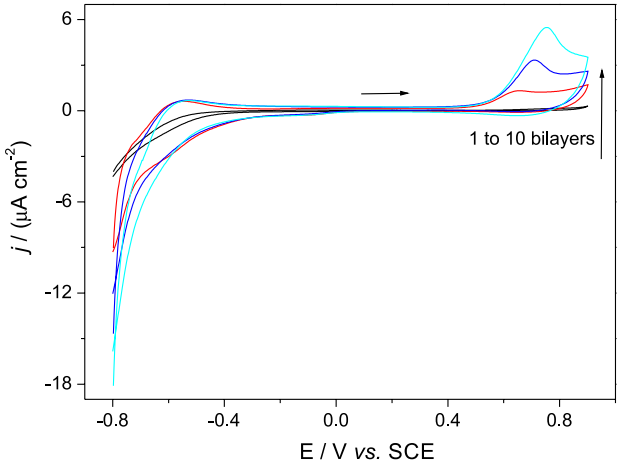

Figure S4. Cyclic voltammograms of the LbL ITO-{Chit-AuNPs/CoTsPc}$_n$ films, where n = 1, 3, 7 and 10 bilayers, in 0.1 mol L^{-1} PBS electrolyte (pH 7.2), scan rate of 0.01 V s^{-1}.

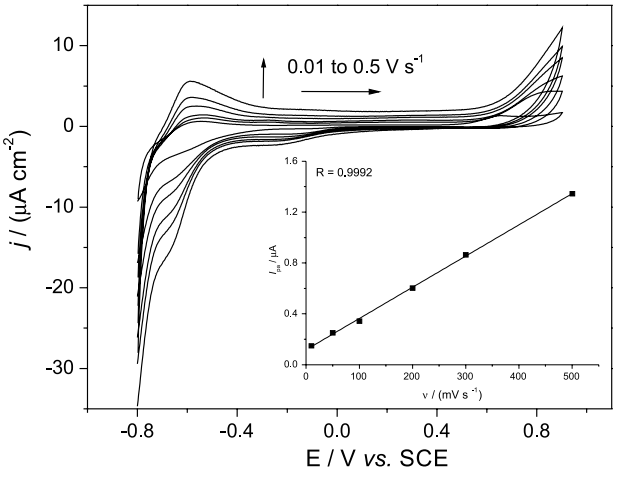

Figure S6. Cyclic voltammograms for the ITO-{Chit-AuNPs/CoTsPc}$_3$ electrode. The inset contains the plot of the anodic peak current (I_{pl} = –0.59 V) *vs.* scan rate (0.01 to 0.5 V s^{-1}). Electrolyte: 0.1 mol L^{-1} PBS solution (pH 7.2), T = 25 °C.

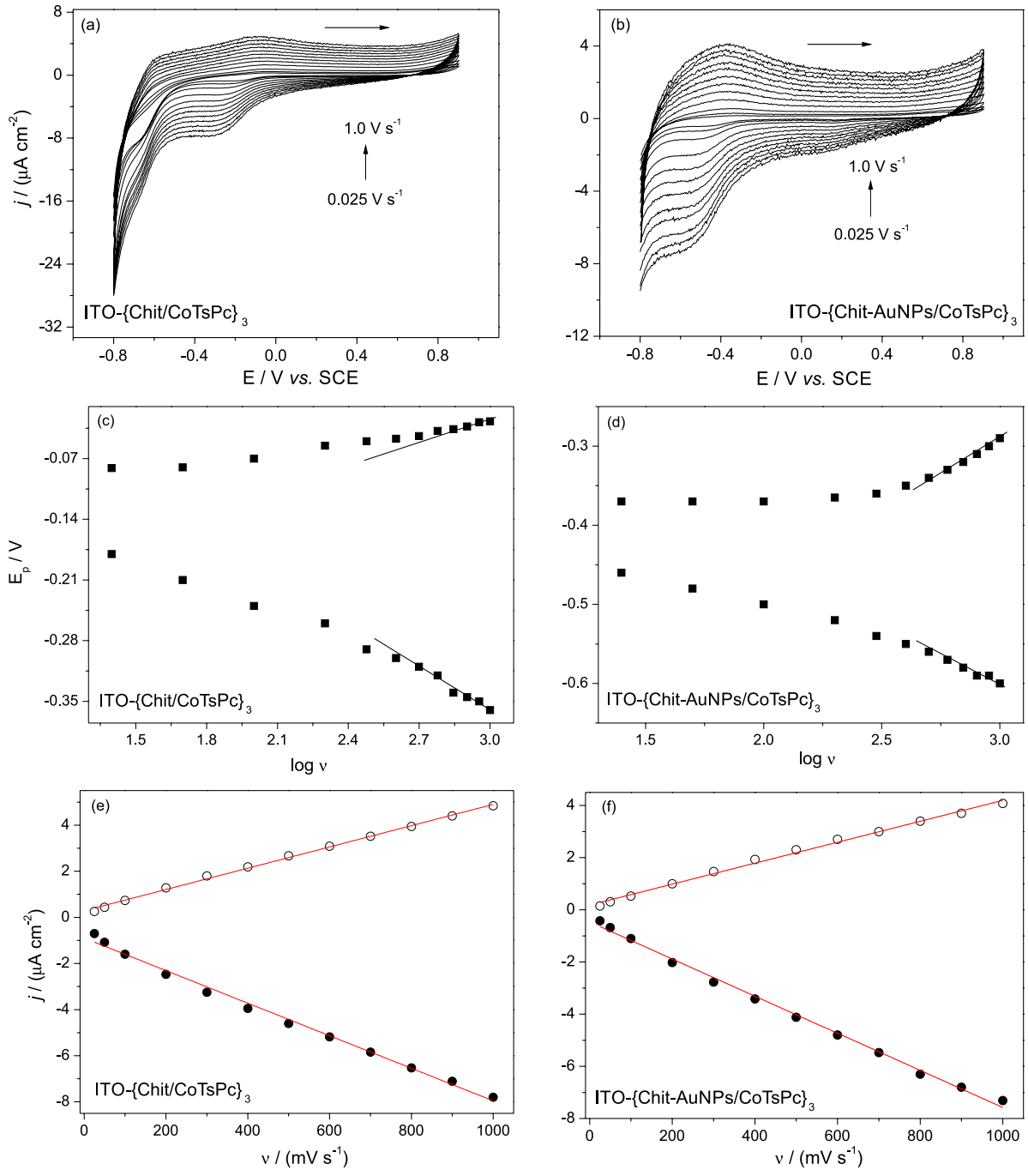

Figure S7. Variation of the scan rate (0.025, 0.050, 0.1, 0.2, 0.3, 0.4, 0.5, 0.6, 0.7, 0.8, 0.9 and 1.0 V s^{-1}) for (a) ITO-{Chit/CoTsPc}$_3$ and (b) ITO-{Chit-AuNPs/CoTsPc}$_3$. Laviron plots for (c) ITO-{Chit/CoTsPc}$_3$ and (d) ITO-{Chit-AuNPs/CoTsPc}$_3$ systems. Dependence of cathodic and anodic peak potentials with scan rates for (e) ITO-{Chit/CoTsPc}$_3$ and (f) ITO-{Chit-AuNPs/CoTsPc}$_3$. Electrolyte: 0.1 mol L^{-1} PBS solution (pH 7.2), T = 25 °C.

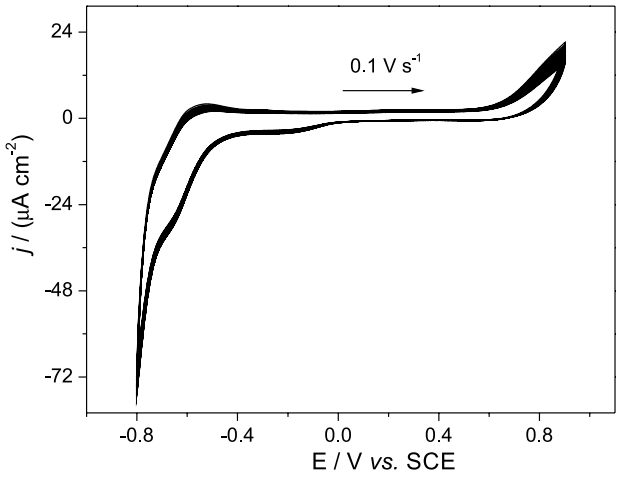

Figure S8. Cyclic voltammograms for the ITO-{Chit-AuNPs/CoTsPc}$_3$ electrode with 20 cycles in 0.1 mol L^{-1} PBS solution (pH 7.2), scan rate of 0.1 V s^{-1}.

Table S1. I_{613}/I_{668} values from UV-Vis spectra for the {Chit-AuNPs/CoTsPc} system

Number of bilayers	I_{613}	I_{681}	I_{613}/I_{668}
1	0.02958	0.01664	1.78
2	0.06774	0.03515	1.93
3	0.10011	0.05195	1.93
5	0.15332	0.08226	1.86
7	0.20652	0.10995	1.88
10	0.27804	0.15036	1.85

Table S2. Average square roughness (R_{ms}) and maximum roughness for the {Chit/CoTsPc}$_n$ and {Chit-AuNPs/CoTsPc}$_n$ films with 1, 3 and 5 bilayers

System	Number of bilayers	Average square roughness / nm	Maximum roughness / nm
{Chit/CoTsPc}$_n$	1	4.40	34.0
	3	8.80	68.0
	5	14.20	108.0
{Chit-AuNPs/CoTsPc}$_n$	1	5.10	45.0
	3	9.60	79.0
	5	14.60	98.0

Table S3. Kinetic parameters for LbL modified electrodes

Electrode	a	k_{ET} / s^{-1}
ITO-{Chit/CoTsPc}$_3$	0.025	0.39
ITO-{Chit-AuNPs/CoTsPc}$_3$	0.08	0.93

α: electrochemical transfer coefficient; k_{ET}: constant of heterogeneous electron transfer.